Graphene Q-switched 0.9-μm Nd:La$_{0.11}$Y$_{0.89}$VO$_4$ laser

Shuo Han (韩 硕), Xianlei Li (李先磊), Honghao Xu (徐洪浩), Yongguang Zhao (赵永光), Haohai Yu (于浩海), Huaijin Zhang (张怀金), Yongzhong Wu (吴拥中), Zhengping Wang (王正平)*, Xiaopeng Hao (郝霄鹏), and Xinguang Xu (许心光)**

State Key Laboratory of Crystal Materials, Shandong University, Jinan 250100, China

**Corresponding author: zpwang@sdu.edu.cn; **corresponding author: xphao@sdu.edu.cn*

Received October 8, 2013; accepted November 19, 2013; posted online December 25, 2013

Graphene saturable absorber (SA) is used as the passive Q-switcher of a 0.9-μm solid-state laser. When the laser medium is a Nd:La$_{0.11}$Y$_{0.89}$VO$_4$ crystal, the initial transmittance of the graphene SA is 78%; at an absorbed pump power of 7.62 W, the maximum average output power, largest pulse energy, and minimum pulse width are 0.62 W, 2.58 μJ, and 84 ns, respectively. This study shows that graphene is a promising and cost-saving SA for 0.9-μm pulse generation.

OCIS codes: 140.3380, 140.3530, 140.3540.
doi: 10.3788/COL201412.011401.

Pulsed laser around 0.9-μm has particular applications in water vapor detection. Second harmonic waves can supply blue laser output, which can be used for underwater optical communication, high-density optical storage, and laser color display.

Graphene can be viewed as a gigantic flat fullerene molecule[1]. It possesses excellent mechanical stiffness, strength, elasticity, and electrical and thermal conductivity[2,3]. Its other advantages are a wide spectral range tunability, ultrafast recovery time, and moderate modulation depth[4−6]. Graphene can function as a saturable absorber (SA) for passive Q-switching and mode locking. In contrast to traditional passive Q-switched devices, such as bulk crystals or semiconductor SA mirrors, graphene can be widely used because of its easy preparation and low cost. To the best of our knowledge, related studies have focused on fiber or solid-state lasers that operate at a range longer than 1 μm[7−15]. The absorption of graphene is slightly dependent on wavelength because of its zero bandgap. Graphene Q-switched laser can operate at 0.9 μm as effectively as it can at 1.06 μm without tuning any material parameters. A short laser pulse can be generated because of the small emission cross section of the gain medium at 0.9 μm. However, no study has examined 0.9-μm Q-switched lasers based on graphene to date.

In this letter, we report nanosecond pulse generation at 0.9 μm from a graphene passively Q-switched Nd-doped crystal laser. At an absorbed pump power of 7.62 W, the maximum average output power, pulse repetition, and minimum pulse width obtained are 0.62 W, 240 kHz, and 84 ns, respectively.

The experimental setup was constructed with a simple plano-concave resonator (Fig. 1). The inner side of the plane mirror, M$_1$, was high reflectivity (HR) coated at 900-950 nm for high transmission (HT) at 808/1064/1340 nm, whereas the outer surface was antireflection (AR) coated at 808 nm. Concave output mirrors, M$_2$, with a radius of 50 mm, were partially reflective (PR) coated at 915 nm with different transmissions (T) of 1%, 5%, and 10%. To obtain a short pulse width, a mixed crystal, Nd:La$_{0.11}$Y$_{0.89}$VO$_4$, which possesses a smaller emission cross section at 0.9 μm than that of Nd:YVO$_4$, was used as the laser medium. Because of the re-absorption losses of a quasi-three-level laser and the large gain for a four-level transition, a 4-mm-long uncoated laser crystal cannot prevent the oscillation of the 1.06-μm spectral line; therefore, the quasi-three-level transition at 0.9 μm was restrained. In this experiment, the 0.3 at.-% Nd^{3+}-doped laser crystal was processed into a relatively short length of 1.5 mm and was a-cut and polished, but it was uncoated. The crystal was wrapped with indium foil and held in a copper block, which was water cooled at a temperature of 8 °C. The SA consisted of five to seven layers of graphene, which were prepared on the surface of a K9 glass substrate, with a corresponding initial transmittance of 78%. The pump source employed was a fiber-coupled laser diode array that produces radiation at 809 nm. The core size of the fiber is 200 μm with a numerical aperture of 0.22. The optical spectrum was measured with an infrared analyzer (SIR 2600, Ocean Optics Inc., USA). The laser pulse signal was detected by a fast photodiode detector (Model D 400 FC, Thorlabs Inc., USA), which was connected to an oscilloscope (DPO 7104, 1 GHz band width and 10 Gs/s sampling rate, Tektronix Inc., USA). The average output power was measured by an energy/power meter (Power Max 500 D, Molectron Inc., USA).

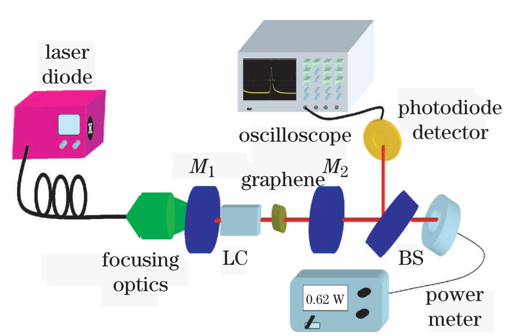

Fig. 1. (Color online) Experimental setup of passively Q-switched Nd:La$_{0.11}$Y$_{0.89}$VO$_4$ laser. LC: laser crystal; BS: beam splitter.

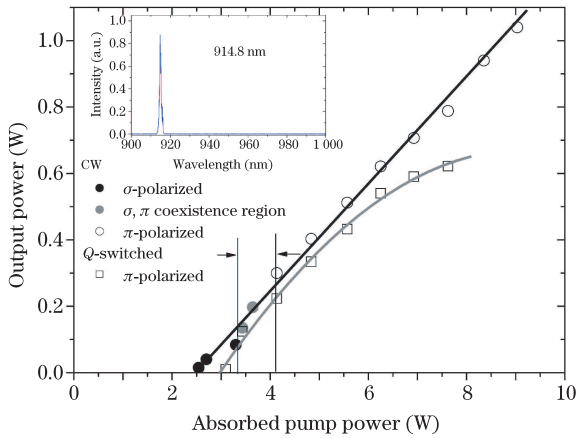

Fig. 2. (Color online) Average output power versus absorbed pump power for continuous wave and Q-switched laser operation. Inset: laser emission spectrum of Nd:$La_{0.11}Y_{0.89}VO_4$ crystal.

In the absence of graphene SA, the continuous wave (CW) laser performance of 915 nm was examined. The cavity length is 48 mm. The thresholds for laser oscillation are reached at absorbed pump powers (P_{abs}) of 1.96, 2.54, and 4.13 W for T = 1%, 5%, and 10%, respectively. The most efficient laser action is obtained with the output coupler of T = 5%; at a pump power of P_{abs} = 9.03 W, an output power of 1.04 W is produced, and it results in an optical-to-optical efficiency of 11.5% and a slope efficiency of 16.0% (Fig. 2). At low pump powers, the laser oscillates in σ polarization. This state remains unchanged until P_{abs} = 3.30 W; at this point, π polarization oscillation occurs. At a pump power range of P_{abs} = 3.30-4.13 W, π and σ polarized lasers coexist. However, when P_{abs} exceeds 4.13 W, only π polarization exists. The effective gain cross section (σ_g) for 915 nm is determined by stimulated emission cross section (σ_{em}), absorption cross section (σ_{abs}), and the fraction of Nd ions excited to the upper manifold (β)[16]:

$$\sigma_g(\lambda) = [\beta\sigma_{em}(\lambda) - (1-\beta)\sigma_{abs}(\lambda)]. \qquad (1)$$

In a relatively low pump level, $\sigma_{abs,\pi}$ is considerably larger than $\sigma_{abs,\sigma}$, and σ polarization oscillation can be first observed for a large $\sigma_{g,\sigma}$. As the pump power increases, i.e., as β increases, the weight of σ_{em} is enhanced, whereas the influence of σ_{abs} is weakened; $\sigma_{g,\pi}$ exceeds $\sigma_{g,\sigma}$ at a high pump level. Laser oscillation undergoes polarization coexistence (π,σ) with single polarization (π) by gain competition.

Tuning the cavity length to 35 mm and inserting the graphene SA increase the oscillating threshold to 3.09 W. The maximum average output power of 0.62 W is obtained under an absorbed pump power of 7.62 W, which corresponds to optical-to-optical and slope efficiencies of 8.1% and 14.0%, respectively. The center wavelength is 914.8 nm (Fig. 2).

Based on the expression of the Q-switched condition, which was derived in Refs. [17,18]:

$$\left|\frac{dR}{dI}\right| > r\frac{T_R}{\tau I}, \qquad (2)$$

where R is the reflectivity of graphene SA, I is the laser intensity, r is the pump parameter that indicates that the laser is pumped above the threshold, T_R is the cavity round-trip time, and τ is the upper-state lifetime of the laser medium. With the results for the five to seven layers of graphene considered[4], the average value of dR/dI is 2.9×10^{-11} m^2/W. To obtain Q-switched laser operation, a long upper-state lifetime (τ) and a short cavity round trip time should be selected. In this experiment, the upper-state lifetime of Nd:$La_{0.11}Y_{0.89}VO_4$ is 103 μs. The cavity round trip time T_R is 233 ps. r and I are estimated to be 2.47 and 1.75×10^8 W/m^2. $rT_R/\tau I$ = 3.19×10^{-14} m^2/W is significantly smaller than 2.9×10^{-11} m^2/W. Therefore, Q-switched operation is observed in the experiment.

Figure 3 shows the dependence of the repetition rate and pulse width on the absorbed pump power. As the absorbed pump power increases, the repetition rate increases from 156 to 240 kHz, whereas the pulse width rapidly decreases from 378 to 84 ns. The maximum frequency of 240 kHz and the minimum pulse width of 84 ns (Fig. 4) are obtained at an absorbed pump power of 7.62 W, which corresponds to a maximum pulse energy of 2.58 μJ and a peak power of 31 W. Graphene Q-switched 0.9-μm Nd:$La_{0.11}Y_{0.89}VO_4$ laser is then realized for the first time. The pulse width of 84 ns is shorter than those of previously reported graphene Q-switched 1.06-μm lasers[13,19].

Figure 5 illustrates a beam profile, which was measured at an output power of 0.62 W for Nd:$La_{0.11}Y_{0.89}VO_4$ laser operating in Q-switched mode. The intensity distribution of the beam profile possesses good symmetry. The beam quality factors M^2 were calculated to be 2.35 and 2.55 for the horizontal and vertical directions, respectively. These measurements correspond to high-order

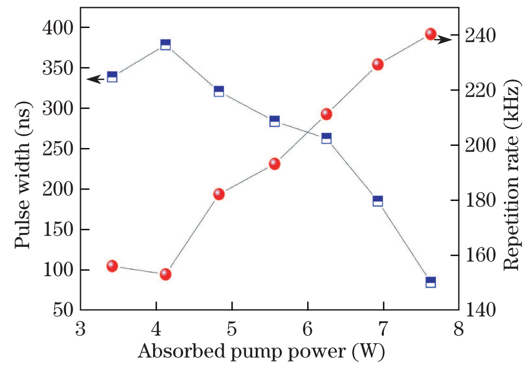

Fig. 3. (Color online) Repetition rate and pulse width versus absorbed pump power for Q-switched laser operation.

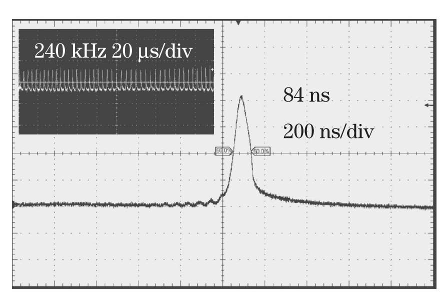

Fig. 4. Pulse profile with a width of 84 ns under an absorbed pump power of 7.62 W. Inset: corresponding pulse train of 240 kHz.

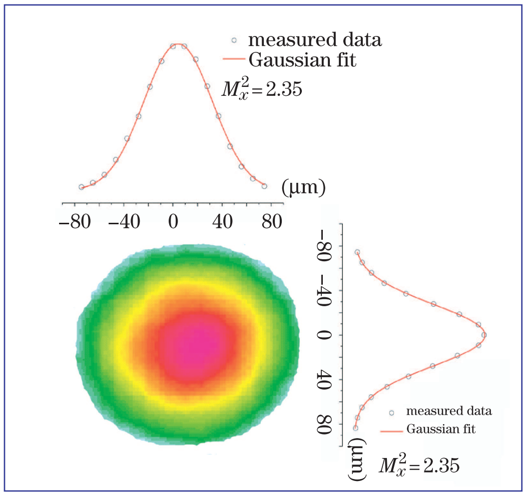

Fig. 5. (Color online) Two-dimensional beam intensity distribution of the graphene Q-switched 0.9-μm laser.

transverse modes. For fundamental mode oscillation, the laser beam radius is calculated to be 80 μm in laser crystal, and the pump beam radius is approximately 100 μm at the same position. With the thermal lensing effect considered, high-order transverse modes can oscillate.

In conclusion, we report a graphene Q-switched 915-nm solid-state laser. The largest pulse energy is 2.58 μJ, and the shortest pulse width is 84 ns. This pulse width is shorter than those obtained in graphene Q-switched 1.06-μm lasers. Optimizing graphene parameters, using an efficient laser medium, and AR coating on a long laser crystal can therefore result in a large output power, high output energy, and short pulse width. This study also proves that graphene is an effective and promising passive Q-switching material for a quasi-three-level laser, which is favorable for large-scale and cost-saving production. Using a nonlinear frequency doubling technique may also help generate an efficient blue-pulsed laser.

This work was supported by the National Natural Science Foundation of China (No. 61178060), the Program for New Century Excellent Talents in the University (No. NCET-10-0552), the Independent Innovation Foundation of Shandong University (No. 2012TS215), and the Natural Science Foundation for Distinguished Young Scholars of Shandong Province (No. 2012JQ18).

References

1. K. S. Novoselov, A. K. Geim, S. V. Morozov, D. Jiang, Y. Zhang, S. V. Dubonos, I. V. Grigorieva, and A. A. Firsov, Science **306,** 666 (2004).
2. A. K. Geim and K. S. Novoselov, Nature Mater. **6,** 183 (2007).
3. A. K. Geim, Science **324,** 1530 (2009).
4. Q. L. Bao, H. Zhang, Y. Wang, Z. H. Ni, Y. L. Yan, Z. X. Shen, K. P. Loh, and D. Y. Tang, Adv. Funct. Mater. **19,** 3077 (2009).
5. Z. P. Sun, T. Hasan, F. Torrisi, D. Popa, G. Privitera, F. Wang, F. Bonaccorso, D. M. Basko, and A. C. Ferrari, ACS Nano **4,** 803 (2010).
6. H. Zhang, D. Y. Tang, R. J. Knize, L. M. Zhao, Q. L. Bao, and K. P. Loh, Appl. Phys. Lett. **96,** 111112 (2010).
7. W. D. Tan, C. Y. Su, R. J. Knize, G. Q. Xie, L. J. Li, and D. Y. Tang, Appl. Phys. Lett. **96,** 031106 (2010).
8. H. Zhang, D. Y. Tang, L. M. Zhao, O. L. Bao, and K. P. Loh, Opt. Express **17,** 17630 (2009).
9. G. Q. Xie, J. Ma, P. Lv, W. L. Gao, P. Yuan, L. J. Qian, H. H. Yu, H. J. Zhang, J. Y. Wang, and D. Y. Tang, Opt. Mat. Express **2,** 878 (2012).
10. Z. B. Liu, X. Y. He, and D. N. Wang, Opt. Lett. **36,** 3024 (2011).
11. J. Liu, S. D. Wu, Q. H. Yang, and P. Wang, Opt. Lett. **36,** 4008 (2011).
12. W. B. Cho, J. W. Kim, H. W. Lee, S. Bae, B. H. Hong, S. Y. Choi, I. H. Baek, K. Kim, D. I. Yeom, and F. Rotermund, Opt. Lett. **36,** 4089 (2011).
13. H. H. Yu, X. F. Chen, H. J. Zhang, X. G. Xu, X. B. Hu, Z. P. Wang, J. Y. Wang, S. D. Zhuang, and M. H. Jiang, ACS Nano **4,** 7582 (2010).
14. Y. K. Yap, Richard M. De La Rue, C. H. Pua, S. W. Harun, and H. Ahmad, Chin. Opt. Lett. **10,** 041405 (2012).
15. H. Ahmad, F. D. Muhammad, M. Z. Zulkifli, and S. W. Harun, Chin. Opt. Lett. **11,** 071401 (2013).
16. J. Liu, X. Mateos, H. Zhang, J. Wang, M. Jiang, U. Griebner, and V. Petrov, Opt. Lett. **31,** 2580 (2006).
17. U. Keller, K. J. Weingarten, F. X. Kärtner, D. Kopf, B. Braun, I. D. Jung, R. Fluck, C. Hönninger, N. Matuschek, and J. A. Au, IEEE J. Sel. Top. Quantum **2,** 435 (1996).
18. H. A. Haus, IEEE J. Quantum Electron. **QE-12,** 169 (1976).
19. Y. G. Zhao, X. L. Li, M. M. Xu, H. H. Yu, Y. Z. Wu, Z. P. Wang, X. P. Hao, and X. G. Xu, Opt. Express **21,** 3516 (2013).